The Photon Counting Histogram in Fluorescence Fluctuation Spectroscopy

Yan Chen,* Joachim D. Müller,* Peter T. C. So,# and Enrico Gratton*

*Laboratory for Fluorescence Dynamics, University of Illinois at Urbana-Champaign, Urbana, Illinois 61801 and #Department of Mechanical Engineering, Massachusetts Institute of Technology, Cambridge, Massachusetts 02139 USA

ABSTRACT Fluorescence correlation spectroscopy (FCS) is generally used to obtain information about the number of fluorescent particles in a small volume and the diffusion coefficient from the autocorrelation function of the fluorescence signal. Here we demonstrate that photon counting histogram (PCH) analysis constitutes a novel tool for extracting quantities from fluorescence fluctuation data, i.e., the measured photon counts per molecule and the average number of molecules within the observation volume. The photon counting histogram of fluorescence fluctuation experiments, in which few molecules are present in the excitation volume, exhibits a super-Poissonian behavior. The additional broadening of the PCH compared to a Poisson distribution is due to fluorescence intensity fluctuations. For diffusing particles these intensity fluctuations are caused by an inhomogeneous excitation profile and the fluctuations in the number of particles in the observation volume $\bar{N}$. The quantitative relationship between the detected photon counts and the fluorescence intensity reaching the detector is given by Mandel's formula. Based on this equation and considering the fluorescence intensity distribution in the two-photon excitation volume, a theoretical expression for the PCH as a function of the number of molecules in the excitation volume is derived. For a single molecular species two parameters are sufficient to characterize the histogram completely, namely the average number of molecules within the observation volume and the detected photon counts per molecule per sampling time ϵ. The PCH for multiple molecular species, on the other hand, is generated by successively convoluting the photon counting distribution of each species with the others. The influence of the excitation profile upon the photon counting statistics for two relevant point spread functions (PSFs), the three-dimensional Gaussian PSF conventionally employed in confocal detection and the square of the Gaussian-Lorentzian PSF for two photon excitation, is explicitly treated. Measured photon counting distributions obtained with a two-photon excitation source agree, within experimental error with the theoretical PCHs calculated for the square of a Gaussian-Lorentzian beam profile. We demonstrate and discuss the influence of the average number of particles within the observation volume and the detected photon counts per molecule per sampling interval upon the super-Poissonian character of the photon counting distribution.

INTRODUCTION

The systematic and quantitative study of fluctuations started at the beginning of this century with the invention of the ultramicroscope. This instrument permitted for the first time the detection and study of particles with a diameter of less than 0.1 μm (Siedentopf and Zsigmondy, 1903). Fluctuation experiments with the ultramicroscope by Perrin and others beautifully confirmed the theory of Brownian motion and diffusion developed by Einstein and Smoluchowski. The results of their experiments contributed significantly to the acknowledgement of the physical reality of the atomistic theory and helped to establish the study of fluctuation phenomena as a new branch of physics. Fluctuation spectroscopy is at present an extremely diverse field with applications ranging from spin glasses and superconductors to biological cells (Braun et al., 1994; Rabin et al., 1998; Weissman, 1993).

Received for publication 18 December 1998 and in final form 15 March 1999.

Address reprint requests to Dr. Yan Chen, Laboratory for Fluorescence Dynamics, University of Illinois at Urbana-Champaign, 184 Loomis Lab, 1110 West Green, Urbana, IL 61801. Tel.: 217-244-5620; Fax: 217-244-7187; E-mail: yan@lfd.physics.uiuc.edu.

0006-3495/99/07/553/15 $2.00

The inherent sensitivity and specificity of fluorescence spectroscopy suit this technique for fluctuation studies, with its requirement of high background rejection and low sample concentration. In the early 1970s Magde, Elson, and Webb (Elson and Magde, 1974; Magde et al., 1972) introduced fluorescence correlation spectroscopy (FCS) and applied the technique to investigation of the diffusion and binding of ethidium bromide to double-stranded DNA. To keep the average number of particles in the observation volume small and at the same time reject the background signal, it becomes necessary to work with small volumes. The implementation of confocal (Qian and Elson, 1991; Rigler et al., 1993a; Koppel et al., 1994) and two-photon microscopy (Berland et al., 1995) with their tiny observation volumes ($V \approx 1\ \mu m^3$) greatly increased the sensitivity of FCS and pushed the detection limit to the single-molecule level (Rigler et al., 1993b; Eigen and Rigler, 1994).

FCS can be used to study kinetic processes, which cause fluctuations in the fluorescence intensity. The time-dependent decay of these fluctuations is characterized by the autocorrelation function $g(\tau)$, which is directly attained from FCS experiments. There are theoretical models for a number of kinetic processes, such as diffusion or chemical reactions (Elson and Magde, 1974; Ehrenberg and Rigler, 1974; Aragon and Pecora, 1975). FCS has been applied to the study of translational and rotational diffusion (Koppel et

al., 1976; Kask et al., 1989), flow (Magde et al., 1978), chemical reactions (Magde et al., 1974), triplet state kinetics (Widengren et al., 1995), hybridization reactions (Kinjo and Rigler, 1995; Schwille et al., 1996), and protein-ligand interactions (Rauer et al., 1996). Kinetic processes on surfaces and in bulk solutions were characterized by FCS (Koppel et al., 1976; Borejdo, 1979; Thompson and Axelrod, 1983). In the case of pure translational diffusion two parameters can be recovered from the autocorrelation function; the average number of molecules $\bar{N}$ in the observation volume, which is inversely proportional to the value of $g(0)$ and the diffusion coefficient D of the particles (Magde et al., 1978; Palmer and Thompson, 1989a).

Besides correlation functions, probability distributions are most commonly used to describe random processes (Bendat and Piersol, 1971). While the temporal behavior of fluctuations is best described by the autocorrelation function, the amplitude of the fluctuations is characterized by its probability distribution. Here we are specifically interested in the probability distribution to detect k photons per sampling time for typical fluorescence fluctuation experiments. This probability is experimentally determined by the histogram of the detected photons, which will be called photon counting histogram (PCH).

The probability to detect k photoelectrons $p(k)$ per sampling time in fluorescence fluctuation experiments has so far received relatively little attention (Qian and Elson, 1989, 1990). In this work we develop a theoretical expression for the photon counting histogram based on the theory of photon detection (Saleh, 1978). The shape of the point spread function (PSF) is taken explicitly into consideration, while allowing Poissonian number fluctuations of the particles in the observation volume. The fluorescence fluctuations caused by a small number of particles in the observation volume yield a super-Poissonian distribution of photon counts. A super-Poissonian distribution has a width that is broader than its mean, whereas for a Poissonian distribution the width and the mean have the same value. We show that for a single chemical species two parameters uniquely characterize the distribution of photon counts, the average number of molecules in the observation volume $\bar{N}$ and the molecular brightness ϵ. The molecular brightness is the average number of detected photons per sampling time per molecule and plays a fundamental role in the statistical accuracy of FCS measurements (Koppel, 1974). The influence of both parameters on the shape of the histogram is discussed.

To test the theory, fluorescence fluctuation experiments with a two-photon microscope were performed. The photon count distribution of fluorescent dyes was measured at different concentrations and compared to the theory. To extract the average number of molecules $\bar{N}$ and the brightness ϵ from the experimental data, a computer algorithm was developed, which fits the experimental PCH to the theory. The same experimental data set determines both the autocorrelation function and the photon counting histogram. For a single species the diffusion is determined by the autocorrelation function and its molecular brightness ϵ by the photon counting histogram. However, the average number of molecules $\bar{N}$ can be recovered by both methods and was used to compare the analysis techniques.

We generalize the theory of the photon counting histogram to a mixture of species and demonstrate it experimentally for the case of two species. Resolving a mixture of species into its components can be a vexing problem in fluorescence fluctuation spectroscopy. The autocorrelation function offers a way to separate species, if their diffusion coefficients differ substantially. PCH analysis offers another way to distinguish between different species, which is based on the difference in brightness between the molecular species and not on the temporal behavior of the fluctuations. Thus PCH analysis can provide information that is not accessible through the autocorrelation function. This capability is a major advantage, inasmuch as the analysis of systems composed of multiple species is ubiquitous in biophysics.

THEORY

In this section we derive an expression for the PCH of freely diffusing molecules and explicitly allow for fluctuations in the number of molecules. To arrive at such a description we first treat the case of a single diffusing particle enclosed in a small volume. The shape of the excitation profile determines the PCH under this condition and will be treated explicitly for two different cases. Subsequently we will expand the model to include more than one diffusing particle in the same enclosed volume. In the last step we remove the boundary volume and develop the theory for an open system with Poissonian number fluctuations. We start by considering the statistics of the photon detection process.

Photon detection

The low light levels typically encountered in FCS experiments require the use of photon counting techniques together with efficient single photon detectors such as photomultiplier tubes (PMTs) or avalanche photodiodes (APDs). The elementary event in the detection process is the generation of a charge separation after the absorption of a photon by the detector. This photon-induced charge is then subsequently amplified to yield an electronic signal. The primary step in the detection process involves the interaction of a photon with matter, which is purely quantum mechanical in nature. However, for most cases a semiclassical description of the detection process, in which the electromagnetic field is treated classically and only the atomic system is described quantum mechanically, is sufficient to cover most experimental situations (Saleh, 1978). The resulting photon counting statistics for the semiclassical case has been worked out and is referred to as Mandel's formula (Mandel, 1958):

$$p(k, t, T) = \int_0^\infty \frac{(\eta_W W(t))^k e^{-\eta_W W(t)}}{k!} p(W(t))\mathrm{d}W(t). \quad (1)$$

The probability $p(k, t, T)$ of observing k photoelectron events at time t depends on the statistical properties of the light reaching the detector, the detection efficiency η_W, and the integration time T. The energy of light falling upon the detector surface is given by the light intensity $I(r, t)$ integrated over the time period T and the detector area A:

$$W(t) = \int_t^{t+T} \int_{\mathbf{A}} I(r, t) \mathrm{d}\mathbf{A}\, \mathrm{d}t. \tag{2}$$

The photon counting distribution $p(k, t, T)$ is thus the Poisson transformation of the energy distribution $p(W(t))$.

From a mathematical point of view, Eq. 1 constitutes a doubly stochastic Poisson point process based on the two sources of randomness encountered (Snyder, 1975). The first is quantum mechanical in nature and reflects the discreteness and statistical independence of the photoelectric detection process for coherent electromagnetic radiation. This fundamental form of noise is also known as shot noise, a random Poisson point process, which cannot be eliminated. Thus even if the light source has absolute constant intensity with $p(W) = \delta(W - \bar{W})$, the resulting photon count distribution due to the shot noise is given by a Poisson distribution,

$$\mathrm{Poi}(k, \langle k \rangle) = \frac{(\eta_W W)^k e^{-\eta_W W}}{k!}. \tag{3}$$

The variance $\langle \Delta k^2 \rangle$ serves as an indicator of the width of a distribution and for the Poisson distribution is equal to its average value, $\langle \Delta k^2 \rangle = \langle k \rangle$.

The second source of noise is fluctuations in the light intensity reaching the detector, which are characterized by the probability distribution $p(W)$. Any fluctuations in the light intensity will cause an additional broadening of the photon counting histogram $p(k, t, T)$ compared to a Poisson distribution (Mandel and Wolf, 1995). This is immediately clear from the structure of Eq. 1, which constitutes a superposition of Poisson distributions for each of the energy values W, with the amplitudes given by the value of $p(W)$. The distribution $p(k, t, T)$ is now characterized by a variance $\langle \Delta k^2 \rangle$ greater than its mean value, $\langle \Delta k^2 \rangle > \langle k \rangle$, which is classified as super-Poissonian (Teich and Saleh, 1988).

A sub-Poissonian distribution is hence analogously defined by a variance $\langle \Delta k^2 \rangle$ smaller than its mean, $\langle \Delta k^2 \rangle < \langle k \rangle$. Mandel's semiclassical formula, however, excludes the existence of sub-Poissonian statistics. It is, nevertheless, possible to generate photon counting histograms with a width narrower than the mean, as first demonstrated in resonance fluorescence experiments (Short and Mandel, 1983). To understand these properties one has to abandon the semiclassical theory and use the corresponding photon counting statistics for the full quantum mechanical case, which was developed by Glauber (1966). The full quantum mechanical description allows new states not covered by the semiclassical theory, including squeezed states of light (Walls, 1983) and photon antibunching (Kimble et al., 1977). However, our current experimental situation is fully described by the semiclassical picture.

As mentioned earlier, the fluctuation of the light intensity $I(t)$ will cause additional broadening of the photon counting histogram $p(k, t, T)$, which depends on the integration time T. In the limit of long integration times, $T \to \infty$, the intensity fluctuations will be completely averaged out in the corresponding fluctuations of the light energy $W(t)$. The probability distribution $p(W)$ approaches a delta function, and the PCH will narrow to a Poissonian. In the other extreme, for very short integration times, $T \to 0$, the energy fluctuations $W(t)$ will completely track the intensity fluctuations $I(t)$. Thus the probability distributions of the energy and intensity are proportional to each other, $p(W) = p(I)\Delta t$. To capture intensity fluctuations of a particular process of interest in the photon counting histogram $p(k, t, T)$, it is mandatory to choose an integration time T shorter than the fluctuation time scale for that particular process. We will assume for the rest of the paper that the integration time T is chosen to be short enough such that the energy fluctuations track the intensity fluctuations of interest. We can thus rewrite Mandel's formula by replacing the energy W with the intensity I_D at the detector:

$$p(k) = \int_0^\infty \frac{(\eta_I I_D)^k e^{-\eta_I I_D}}{k!} p(I_D) \mathrm{d}I_D = \int_0^\infty \mathrm{Poi}(k, \eta_I I_D) p(I_D) \mathrm{d}I_D. \tag{4}$$

For simplicity, we take the detector area A as small enough, so that the intensity field I is constant across the detector surface with a short sampling time interval of $T = \Delta t$. We also assumed a stationary process, so that there is no time dependence to the statistical properties of the fluctuating light intensity I and therefore no time dependence to the photon counting histogram $p(k)$. The new constant η_I is proportional to the detection efficiency η_W and takes the sampling time $T = \Delta t$ into account, $\eta_I = T\eta_W$.

Point spread function

The small excitation volume generated by the microscope optics allows the effective observation of fluorescence intensity fluctuations. The spatial intensity distribution of the excitation light is characterized by its PSF. In our context it is more convenient to define a scaled PSF:

$$\overline{\mathrm{PSF}}(x, y, z) = \frac{\mathrm{PSF}(x, y, z)}{\mathrm{PSF}(0, 0, 0)}, \tag{5}$$

which is normalized at the origin.

For our experimental two-photon setup, the PSF is well approximated by the square of the Gaussian-Lorentzian beam profile (Berland et al., 1995):

$$\overline{\mathrm{PSF}}_{2GL}(\rho, z) = \frac{I^2(\rho, z)}{I_o^2} = \frac{4\omega_o^4}{\pi^2 \omega^4(z)} \exp\left[-\frac{4\rho^2}{\omega^2(z)} \right]. \tag{6}$$

The PSF is expressed in cylindrical coordinates for an excitation wavelength λ and a beam waist of the excitation profile ω_o. The inverse of the Lorentzian along the optical axis is given by

$$\omega^2(z) = \omega_0^2\left(1 + \left(\frac{z}{z_R}\right)^2\right), \quad \text{with } z_R = \frac{\pi\omega_o^2}{\lambda}. \tag{7}$$

Another important case is confocal detection, where the depth discrimination is achieved via a pinhole at the detector. The PSF in confocal spectroscopy is given by the convolution of the excitation PSF, and the detection PSF and has been considered in detail (Qian and Elson, 1991). It was shown that concerning FCS, the PSF is nevertheless well approximated by a three-dimensional Gaussian (Rigler et al., 1993a):

$$\overline{\mathrm{PSF}}_{3DG}(x, y, z) = \frac{I(x, y, z)}{I_0} = \exp\left[-\frac{2(x^2 + y^2)}{\omega_0^2} - \frac{2z^2}{z_0^2}\right], \tag{8}$$

with an effective beam waist z_0 in the axial direction.

The fluorescence intensity I_D at the detector for a fluorophore at position $\vec{r}_0$ is given by the PSF and the excitation intensity I_0 at the center of the PSF:

$$I_D = I_0^n\beta\overline{\mathrm{PSF}}(\vec{r}_0). \tag{9}$$

For two-photon excitation the fluorescence intensity is proportional to the square of the excitation intensity ($n = 2$), whereas for normal excitation it is proportional to the excitation intensity ($n = 1$). The coefficient β contains the excitation probability, the fluorescence quantum yield, and all of the instrument-dependent factors, such as the transmittance of the fluorescence through the microscope optics and the quantum yield of the detector.

PCH for a single particle

To model the photon counting histogram of fluorescence fluctuations, we need to combine the PSF with Mandel's formula. Equation 9 connects the intensity at the detector with the position $\vec{r}$ of a fluorescent particle. Thus we can express the probability $p(I_D)$ with the help of Eq. 9 as

$$p(I_D) = \int \delta(I_D - I_0^n\beta\overline{\mathrm{PSF}}(\vec{r}))p(\vec{r})\mathrm{d}\vec{r}, \tag{10}$$

where the transformation property of probabilities was applied (van Kampen, 1981). Before we insert Eq. 10 into Mandel's formula, we need to choose the appropriate probability distribution $p(\vec{r})$. Let us assume a single particle enclosed within a volume V_0. The particle can diffuse freely within the bounds of the volume V_0. Because the particle can be found with equal probability at any position within the volume V_0, the probability $p(\vec{r})$, if $\vec{r}$ is within the volume, is simply given by the inverse of the total volume and is zero otherwise:

$$p(\vec{r}) = \begin{cases} 1/V_0, & \text{for } \vec{r} \in V_0 \\ 0, & \text{for } \vec{r} \notin V_0 \end{cases}. \tag{11}$$

Inserting the probability $p(\vec{r})$ and Eq. 10 into Mandel's formula (Eq. 4) yields the following result:

$$\begin{aligned} p^{(1)}(k; V_0, \epsilon) &= \int \mathrm{Poi}(k, \epsilon\overline{\mathrm{PSF}}(\vec{r}))p(\vec{r})\mathrm{d}\vec{r} \\ &= \frac{1}{V_o}\int_{V_o} \mathrm{Poi}(k, \epsilon\overline{\mathrm{PSF}}(\vec{r}))\mathrm{d}\vec{r}, \end{aligned} \tag{12}$$

where ϵ is given by $\epsilon = I_0^n\beta\eta_I$. Equation 11 is the fundamental equation for determining the PCH $p^{(1)}(k; V_0, \epsilon)$ for a single molecule. It is the weighed average of Poissonian distributions, each with a mean of $\epsilon\overline{\mathrm{PSF}}(\vec{r})$, over the volume V_0. If we consider, instead of a freely diffusing particle, a particle fixed at position $\vec{r}_0$, the resulting PCH yields a Poissonian with a mean of $\epsilon\overline{\mathrm{PSF}}(\vec{r}_0)$:

$$p^{(\mathrm{fixed})}(k, r_0) = \mathrm{Poi}(k, \epsilon\overline{\mathrm{PSF}}(\vec{r}_0)). \tag{13}$$

The average photon count $\langle k\rangle$ of the PCH $p^{(1)}(k; V_0, \epsilon)$ is given by

$$\langle k\rangle = \frac{\epsilon}{V_0}\int_{V_0} \overline{\mathrm{PSF}}(\vec{r})\mathrm{d}\vec{r} = \epsilon\frac{V_{\mathrm{PSF}}}{V_0}. \tag{14}$$

The average photon counts are essentially determined by the parameter ϵ and the probability of finding the molecule within the volume of the point spread function $p = V_{PSF}/V_0$. The molecular brightness $\epsilon = I_0^n\beta\eta_W T$ scales with the sampling time T, but the ratio $\epsilon_{sec} = \epsilon/T$ is independent of the arbitrary sampling time T. The new parameter ϵ_{sec} can be used to express the brightness in counts per second per molecule (cpsm) and allows a more convenient comparison between experiments.

Now we will explicitly calculate the probability distribution for a single molecule according to Eq. 12 for the two point spread functions discussed earlier. For mathematical convenience we will integrate Eq. 12 over all space, but still reference to a volume V_0. Because the reference volume V_0 is chosen so that the PSF is essentially contained within it, there are no additional photons excited outside of the reference volume V_0, and the change in the probability $p^{(1)}(k; V_0, \epsilon)$ caused by the change in the integration limits to infinity are negligible except for $k = 0$. Outside the PSF no photons will be generated, and the additional contributions made by changing the integration limits lead to the divergence of the integral for $k = 0$. The probability $p^{(1)}(0; V_0, \epsilon)$ of receiving no photon counts is simply determined by using the normalization condition of probability distributions, so that $p^{(1)}(0; V_0, \epsilon) = 1 - \sum_{k=1}^{\infty} p^{(1)}(k; V_0, \epsilon)$. The following

equations are all derived by integrating over all space and are only applicable for $k > 0$. Note that the probability $p^{(1)}(k; V_0, \epsilon)$ of receiving k photon counts for a reference volume V_0 is just an intermediate step in deriving an expression for the probability of an open system with fluctuations in the particle number. As expected, the choice of the reference volume V_0 is of no consequence for the final probability of an open system, as will be shown later.

Now we can determine the PCH for a single molecule and a particular PSF of interest. Let us first focus on the case of two-photon excitation, where our PSF can be approximated by the square of a Gaussian-Lorentzian. We insert Eq. 6 into Eq. 12, integrate analytically over ρ, and simplify the expression for the PCH of a single particle to a one-dimensional integral:

$$p^{(1)}_{2GL}(k; V_0, \epsilon) = \frac{1}{V_0}\frac{\pi^2\omega_o^4}{2\lambda k!}\int_0^\infty (1+x^2)\gamma\left(k, \frac{4\epsilon}{\pi^2(1+x^2)^2}\right)dx, \quad \text{for } k > 0. \quad (15)$$

The integral, which contains the incomplete gamma function γ, can be numerically evaluated.

The second case we will consider is for the three-dimensional Gaussian PSF. Again, inserting the equation for the PSF (Eq. 8) into Eq. 12, an analytical integration leads to the PCH in the form of a one-dimensional integral,

$$p^{(1)}_{3DG}(k; V_0, \epsilon) = \frac{1}{V_0}\frac{\pi\omega_0^2 z_0}{k!}\int_0^\infty \gamma(k, \epsilon e^{-2x^2})dx, \quad \text{for } k > 0. \quad (16)$$

PCH for several particles

So far we have only considered the case of a single diffusing molecule. To treat the case for two independent particles of the same species diffusing within an enclosed volume V_0, we simply need two position coordinates $\vec{r}_1$ and $\vec{r}_2$ to account for both particles. The PCH for two independent particles can be described as

$$p^{(2)}(k; V_0, \epsilon) = \iint \mathrm{Poi}(k, \epsilon\overline{\mathrm{PSF}}(\vec{r}_1) + \epsilon\overline{\mathrm{PSF}}(\vec{r}_2))p(\vec{r}_1)p(\vec{r}_2)d\vec{r}_1\, d\vec{r}_2. \quad (17)$$

Essentially to determine the PCH for two independent particles $p^{(2)}(k; V_0, \epsilon)$, the Poisson function associated with the combined intensity of both particles at the detector is averaged over all possible spatial configurations. It is straightforward to generalize the two-particle case to describe N particles. The PCH for N independent particles $p^{(N)}(k; V_0, \epsilon)$ is given by

$$p^{(N)}(k; V_0, \epsilon) = \int\cdots\int d\vec{r}_1\, d\vec{r}_2 \cdots d\vec{r}_N p(\vec{r}_1)p(\vec{r}_2)\cdots p(\vec{r}_N) \mathrm{Poi}\left(k, \epsilon\sum_{i=1}^{N}\overline{\mathrm{PSF}}(\vec{r}_i)\right). \quad (18)$$

Because the PCH $p^{(N)}(k; V_0, \epsilon)$ for the N-particle case has $3N$ integration variables, the evaluation of Eq. 18 becomes computationally formidable. However, if the particles are noninteracting, then we can treat them as statistically independent variables. We can therefore exploit the fact that the moment-generating function for the sum of statistically independent variables is given by the product of the moment-generating functions for each stochastic variable (van Kampen, 1981). Thus the probability distribution for the sum of statistically independent variables is the convolution of the probability distribution of the individual stochastic variables (Feller, 1957). The PCH for two independent particles is therefore given by the convolution of the PCH for the one particle case with itself,

$$p^{(2)}(k; V_0, \epsilon) = (p^{(1)} \otimes p^{(1)})(k; V_0, \epsilon) = \sum_{r=0}^{\infty} p^{(1)}(k-r; V_0, \epsilon)p^{(1)}(r; V_0, \epsilon). \quad (19)$$

By repeating the convolution of the probability distribution $p^{(1)}(k; V_0, \epsilon)$ N-times the PCH for N identical, but independent particles can be generated,

$$p^{(N)}(k; V_0, \epsilon) = \underbrace{(p^{(1)} \otimes \cdots \otimes p^{(1)})}_{\text{N-times}}(k; V_0, \epsilon). \quad (20)$$

Constructing the N-particle PCH $p^{(N)}(k; V_0, \epsilon)$ by convolution of multiple single particle PCH $p^{(1)}(k; V_0, \epsilon)$ according to Eq. 20 is equivalent to the evaluation of the $3N$-dimensional integral, but computationally much more advantageous.

PCH for an open system

So far we have considered the case of particles diffusing within an enclosed volume V_0. In the experiments under consideration, we have an open system with particles entering and leaving the subvolume V_0. We choose the reference volume V_0, so that it is much smaller than the reservoir, and the number fluctuations of the particles are therefore governed by Poisson statistics (Chandrasekhar, 1943):

$$p_{\#}(N) = \mathrm{Poi}(N, \bar{N}), \quad (21)$$

where N is the actual number of particles within the reference volume V_0. The average number of molecules $\bar{N}$ is connected to the concentration c of particles in solution with the help of Avogadro's number N_A as $\bar{N} = cV_0N_A$.

Before we continue we need to describe the photon count probability $p^{(0)}(k; V_0, \epsilon)$ of having no particle present in the volume V_0. If there are no particles present, we receive no photon counts by definition, and the photon count probability is given by

$$p^{(0)}(k; V_0, \epsilon) = \delta(k), \quad \text{with } \delta(k) = \begin{cases} 1, & k = 0 \\ 0, & k > 0 \end{cases}. \tag{22}$$

In the final step in determining the PCH for an open system, we average the individual probability functions for N particles $p^{(N)}(k; V_0, \epsilon)$ weighted by their Poissonian probability of observing N particles $p_{\#}(N)$,

$$\Pi(k; \bar{N}_{PSF}, \epsilon) \equiv \hat{p}(k; V_0, \bar{N}, \epsilon) = \langle p^{(N)}(k; V_0, \epsilon)\rangle_N = \sum_{N=0}^{\infty} p^{(N)}(k; V_0, \epsilon) p_{\#}(N). \tag{23}$$

The function $\hat{p}(k; V_0, \bar{N}, \epsilon)$ describes the probability of observing k photon counts in an open system for a particle solution with a concentration of $c = \bar{N}/(V_0 N_A)$. We will show in Appendix A that the photon count probability of an open system is independent of the reference volume V_0. Thus the photon count probability of an open system should either be referenced to the concentration, which is an intensive quantity and independent of the arbitrary volume V_0, or be referenced to a standard volume with an inherent physical meaning. Here we will follow the convention used in FCS, where the volume of the PSF V_{PSF} (see Eq. 14) serves as the standard volume for connecting the number of molecules $\bar{N}_{PSF}$ with the $g(0)$ value of the autocorrelation function (Thompson, 1991). Therefore we define the PCH function $\Pi(k; \bar{N}_{PSF}, \epsilon)$ for an open volume in Eq. 23, where $\bar{N}_{PSF}$ is the average number of molecules inside the volume of the PSF V_{PSF}. The change from $\bar{N}$ to $\bar{N}_{PSF}$ in Eq. 23 reflects the difference in the reference volume and is determined by the concentration, $c = \bar{N}_{PSF}/(V_{PSF} N_A) = \bar{N}/(V_0 N_A)$. The average number of photon counts $\langle k\rangle$ for an open system can be obtained directly from $\Pi(k; \bar{N}_{PSF}, \epsilon)$ and is simply the product of the brightness per molecule ϵ and the average number of molecules inside the PSF volume $\bar{N}_{PSF}$,

$$\langle k\rangle = \epsilon \bar{N}_{PSF}. \tag{24}$$

PCH for multiple independent species

For more than one chemical species, we have to take the differences in the molecular properties, like the excitation probability, or the quantum yield into account and, in addition, consider the microscope and detector properties for the different emission wavelengths. All of these differences can be absorbed in the coefficient ϵ, which will differ from species to species. The PCH for two species with N_1 particles of brightness ϵ_1 and N_2 particles of brightness ϵ_2 enclosed within a volume V_0 is given by

$$p^{(N_1, N_2)}(k; V_0, \epsilon_1, \epsilon_2) = \int \cdots \int d\vec{r}_i p(\vec{r}_i) \cdots d\vec{r}_j p(\vec{r}_j) \, \mathrm{Poi}\left(k, \epsilon_1 \sum_{i=1}^{N_1} \overline{PSF}(\vec{r}_i) + \epsilon_2 \sum_{j=1}^{N_2} \overline{PSF}(\vec{r}_j)\right). \tag{25}$$

But because the species are assumed to be independent, we can also express the PCH for a mixture as the convolution between the PCH functions of individual species. For the case of an open system we simply convolute the PCH function $\Pi(k; \bar{N}_1, \epsilon_1)$ of species 1 with the equivalent function $\Pi(k; \bar{N}_2, \epsilon_2)$ of species 2 to arrive at the photon count distribution of the mixture,

$$\Pi(k; \bar{N}_1, \bar{N}_2, \epsilon_1, \epsilon_2) = \Pi(k; \bar{N}_1, \epsilon_1) \otimes \Pi(k; \bar{N}_2, \epsilon_2), \tag{26}$$

where $\bar{N}_1$ and $\bar{N}_2$ represent the average number of particles inside the PSF volume V_{PSF}. For more than two independent moving species, the photon counting histograms of all individual components have to be convoluted successively.

MATERIALS AND METHODS

Instrumentation

The instrumentation for two-photon fluctuation experiments is similar to that described by Berland et al. (1995), with the following modifications. The experiments were carried out using a Zeiss Axiovert 135 TV microscope (Thornwood, NY) with a 40× Fluar oil immersion objective (NA = 1.3). A mode-locked Ti:sapphire laser (Mira 900; Coherent, Palo Alto, CA) pumped by an Innova 410 argon ion laser (Coherent) was used as the two-photon excitation source. For all measurements, an excitation wavelength in the range from 770 to 780 nm was used, while the average power at the sample ranged from 15 to 25 mW. Under our experimental conditions no photobleaching was detected for any of the samples measured. Photon counts were detected with either a PMT (R5600-04-P; Hamamatsu) or an APD (SPCM-AQ-161; EG&G). The PMT output was amplified (model 6931; Phillips Scientific, Ramsey, NJ), and a discriminator (model 6930; Phillips Scientific) converted the amplified signal to TTL pulses, which were collected continuously by a home-built computer acquisition card and stored in memory. The output of the APD unit, which produces TTL pulses, was directly connected to the data acquisition card. The photon counts were sampled either at 20 kHz or at 1 kHz. The recorded and stored photon counts were later analyzed with PV-WAVE version 6.10 (Visual Numerics).

Sample preparation

Rhodamine 110, 3-cyano-7-hydroxycoumarin, fluorescein, and yellow-green fluorescent latex microspheres with a diameter of 500 nm were purchased from Molecular Probes (Eugene, OR). All dyes were dissolved in 50 mM Tris[hydroxymethy]amino-methane (Sigma, MO), and the pH was adjusted to 8.5 by adding HCl. Latex spheres were suspended in deionized water. Dye concentrations were determined by absorption measurements, using the extinction coefficients provided by Molecular Probes. Samples were either mounted in hanging drop microscope glass slides or in a plastic sample holder with a window made from a standard microscope cover glass.

Data analysis

The theoretical photon counting distribution $\Pi(k; \bar{N}, \epsilon)$ is determined by numerical integration of the probability density $p^{(1)}(k; V_{PSF}, \epsilon)$ for a particular PSF (Eq. 15 or 16) and $k \geq 1$. The normalization to the volume V_{PSF} allows the determination of $p^{(1)}(0; V_{PSF}, \epsilon)$. After convoluting the density function $p^{(1)}(k, V_{PSF}, \epsilon)$ according to Eq. 20 to obtain $p^{(N)}(k; V_{PSF}, \epsilon)$, the final probability function for an open system with an average of $\bar{N}$ particles in the reference volume V_{PSF} can be determined by weighing $p^{(N)}(k; V_{PSF}, \epsilon)$ according to Eq. 23 with the Poissonian number probability $\mathrm{Poi}(N, \bar{N})$.

The histogram of the experimental data is calculated and then normalized to yield the experimental photon counting probability density $\tilde{p}(k)$. Because a typical data set contains on the order of 10^6 data points, the values of the photon counting density $\tilde{p}(k)$ vary over several orders of magnitude. To fit to the PCH model, we must assign the proper statistical uncertainty to each value of the histogram. For each measurement the probability of yielding k counts is given by the probability $\tilde{p}(k)$ and the complementary probability $\tilde{q}(k) = 1 - \tilde{p}(k)$ of not yielding k counts. The probability of observing k counts r times out of M trials is given by a binomial distribution function $B(r, M, \tilde{p}(k))$, where $\tilde{p}(k)$ is the probability of observing k counts. The expectation value $\langle r \rangle$ for the binomial distribution is given by $\langle r \rangle = M\tilde{p}(k)$ and the standard deviation σ by $\sigma = \sqrt{M\tilde{p}(k)\tilde{q}(k)}$. We weigh each element of the photon counting histogram with its corresponding σ, calculate the theoretical density function $\Pi(k; \bar{N}, \epsilon)$, and then determine the reduced χ^2-function,

$$\chi^2 = \frac{\sum_{k=k_{min}}^{k_{max}} \left(M \frac{\tilde{p}(k) - \Pi(k; \bar{N}, \epsilon)}{\sigma} \right)^2}{k_{max} - k_{min} - d}. \qquad (27)$$

The experimental photon counts range from a minimum value k_{min}, which is typically 0 for most experiments, to a maximum number k_{max}. The number of fitting parameters is given by d. Because we take on the order of $M = 10^6$ data points, the resulting binomial distribution, except for $\langle r \rangle \approx 1$, is well approximated by a normal distribution. Thus the quality of the model can be estimated by the reduced χ^2 and by the normalized residuals of the fit

$$r(k) = M \frac{\tilde{p}(k) - \Pi(k; \bar{N}, \epsilon)}{\sigma}.$$

RESULTS

The photodetection process is sensitive to intensity fluctuations. To determine the intensity fluctuations of the sample alone, an excitation source with constant light intensity is needed. To test this condition, a small fraction of the impinging laser light was scattered onto the detector. The resulting PCH is plotted in Fig. 1 in a linear and semilogarithmic plot. We also calculated the Poisson distribution, using the average photon counts $\langle k \rangle$ as the mean. The PCH of the laser light is well described by a Poisson distribution, and the assumption that the excitation light has a constant excitation intensity as assumed in the Theory section is valid.

In the next measurement a fluorescent particle of 500-nm diameter was immobilized on a glass coverslip. The laser light was focused on the particle to excite two-photon fluorescence. The histograms of the photon counts in Fig. 2 are again described by a Poisson distribution with a mean determined by the average photon counts $\langle k \rangle$. The size of the particle is of the same magnitude as the PSF; therefore the fluorescent particle experiences an inhomogeneous excitation profile. The fluorescence intensity of the particle is the summed contribution of the particle's immobilized fluorophores, which leads to a constant fluorescence intensity with

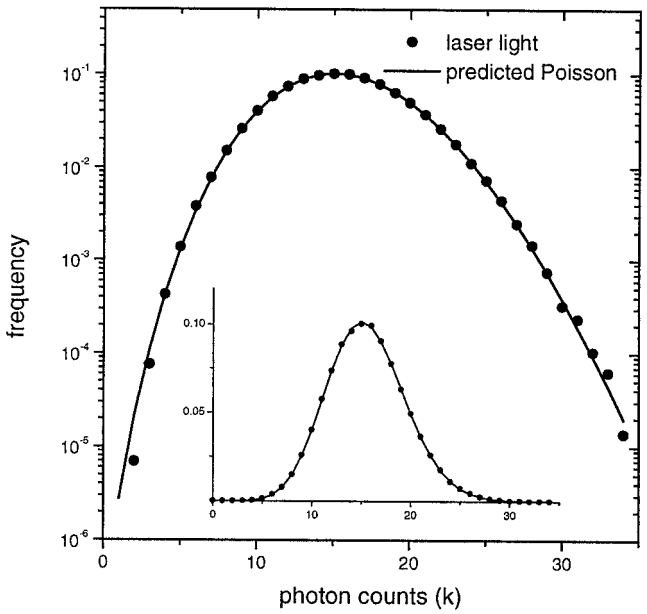

FIGURE 1 Photon counting histogram (●) of the excitation light from a mode-locked Ti:sapphire laser at 780 nm, shown in a semilogarithmic plot. The solid line represents the Poisson distribution with a mean equal to the average photon counts $\langle k \rangle$ of the experimental data. The inset displays the same data in a linear scale for comparison.

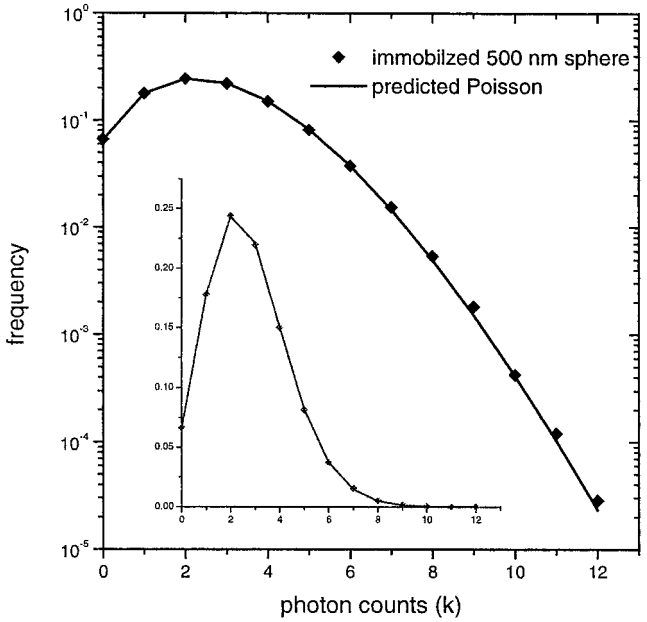

FIGURE 2 Photon counting histogram (◆) of an immobilized fluorescent latex sphere with a diameter of 500 nm. The Poisson distribution (*solid line*) was calculated by using the mean value of the experimental photon counts. The data are displayed in both a semilogarithmic and a linear scale.

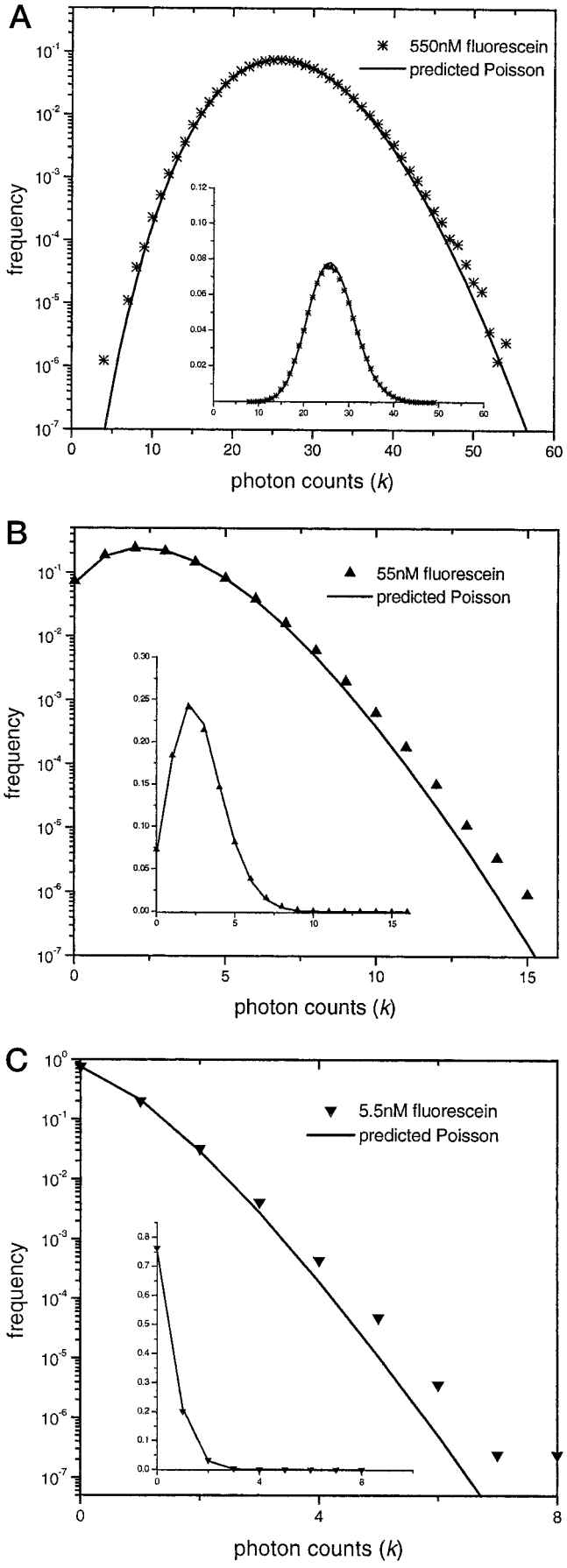

time. The situation is analogous to measuring the laser intensity, but instead of scattered light a fluorescent sphere is used as the light source. To observe a Poissonian photon count distribution, the particle has to remain immobilized during the experiment. Any movement of the particle will lead to intensity fluctuations at the detector and subsequently to a broadening of the photon count distribution.

The above measurements demonstrate that the detected photon counts of the emitted fluorescence under constant excitation light conditions exhibit a Poissonian distribution. The concentration fluctuations of a small volume are also governed by Poissonian statistics; therefore one might first naively expect that the photon counts of diffusing particles will also follow a Poisson distribution. In Fig. 3 the experimentally determined PCHs of the dye fluorescein are shown for three different concentrations in a semilogarithmic plot. The Poisson distribution with a mean equal to the experimental average counts $\langle k \rangle$ is displayed for each histogram as a solid line. The recorded PCH for a dye concentration of 550 nM (Fig. 3 *A*) reaches almost 60 counts per sampling period, with an average of $\langle k \rangle \approx 26$ counts. A Poisson distribution with the same average as the experimental photon counts approximates the data. However, decreasing the dye concentration yields PCHs that are not described by Poisson statistics. At a fluorescein concentration of 55 nM (Fig. 3 *B*), a broadening of the experimental PCH compared to the Poisson distribution is observed. The deviation is clearly visible in the tail of the distribution, which corresponds to high photon counts. Here, the actual experimental data exceed the values based on the Poisson distribution. The deviation of the PCH from the Poisson distribution becomes even more apparent with a reduction in the fluorescein concentration to 5.5 nM (Fig. 3 *C*). In this case the experimental values of the histogram exceed the corresponding values of the Poisson distribution for more than two photon counts.

Each histogram is also displayed as an inset in Fig. 3, which uses a linear scale. In this representation no deviation between the experimental data and a Poisson distribution is detectable by visible inspection, except for the high concentration case ($c = 550$ nM). Because each histogram is based on more than 10^6 data points, the histogram values of the

FIGURE 3 Comparison of the photon counting histogram for fluorescein at different concentrations with the Poisson distribution. Fluorescein was dissolved in 75% glycerol/25% Tris buffer solution (v/v). The samples were measured with a 63× Plan Apochromat objective (NA = 1.4) and an incident laser power at the sample of ~7 mW. The histograms for fluorescein at concentrations of (*A*) 550 nM, (*B*) 55 nM, and (*C*) 5.5 nM are plotted together with their Poisson distribution for a mean equal to the corresponding average photon counts $\langle k \rangle$ of the experimental histogram (Table 1). For the highest concentration only small deviations from a Poisson distribution are noticeable. Lowering the concentration of the fluorescein results in increased deviations of the histogram from a Poisson distribution, as shown in *B* and *C*. This deviation of the experimental data from the Poisson distribution is much more pronounced in the logarithmic representation as compared to the linear scale (shown in the *inset*).

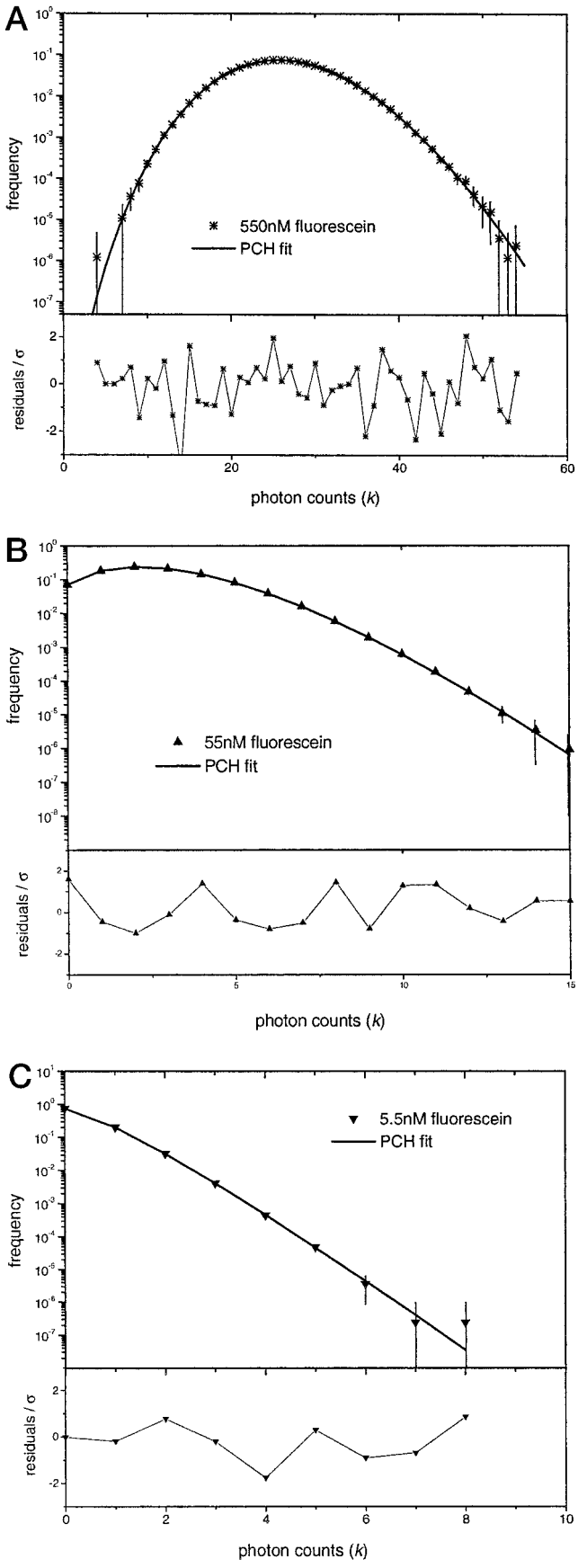

FIGURE 4 Photon counting histogram for fluorescein at three different concentrations, (*A*) 550 nM, (*B*) 55 nM, and (*C*) 5.5 nM. The same histograms as used in Fig. 3 are plotted as symbols, together with an error bar ($\pm 3\sigma$), for each data point on a semilogarithmic scale. The three data sets were fit by globally linking the molecular brightness parameter ϵ across the data sets, while allowing the average number of molecules $\bar{N}$ to vary. The solid line represents the best fit obtained by using the theoretical PCH function $\Pi(k; \bar{N}, \epsilon)$ as explained in the text. The fitting parameters are compiled in Table 1. The lower panel displays the normalized residuals of the fit.

PCH can span six orders of magnitude. A logarithmic scale for the histogram values is therefore essential for picking up the deviations from a Poisson distribution.

In the next step we will reanalyze the same experimental data sets and model them using the PCH for a Gaussian-Lorentzian beam profile, as explained in the Theory section. The corresponding PCH can then be determined by using a fitting algorithm as outlined in Materials and Methods. Each histogram for a single species is characterized by two parameters: the average number of particles $\bar{N}$ in the volume V_{PSF} of the PSF and the average molecular brightness ϵ. Because the three data sets were recorded under the same conditions, except that the fluorescein concentration was varied, the average counts per particle ϵ are the same for all three experiments. We performed a global fit of all three histograms with ϵ linked together across all data sets, while the average number of particles was allowed to vary. The data and the fitted histograms for the three different concentrations in Fig. 4 are in good agreement. The residuals between data and fit for each histogram are displayed in Fig. 4, with each unit representing the standard deviation σ as explained in Materials and Methods. The residuals are random across the counts k and the reduced χ^2 is close to 1, indicating a good description of the data by the theoretical model. The fit parameters and the average counts are compiled in Table 1. The recovered number of molecules $\bar{N}$ scales exactly with the average photon counts $\langle k \rangle$ as predicted by Eq. 24. However, the ratio of both parameters, $\langle k \rangle$ and $\bar{N}$, for each successive dilution is 9.7 instead of 10, as expected for the dilution experiment, thus suggesting an overestimation of the experimental dilution factor.

In a similar experiment we diluted a stock solution of the dye rhodamine 110 successively and measured the photon counts as a function of time. The data of each experiment were analyzed using both the PCH and autocorrelation methods. The average number of molecules $\bar{N}$ was determined by fitting the autocorrelation function $g(\tau)$ as described by Berland et al. (1995). The results of both analysis methods are compiled in Table 2. The average number of photon counts $\langle k \rangle$ scales exactly with the number of molecules $\bar{N}$ based on the PCH analysis and to a lesser extent with the $\bar{N}$ from the autocorrelation function. Nevertheless, both methods are able to recover the average number of molecules in the observation volume V_{PSF}.

We used three different fluorophores, each with its own brightness parameter ϵ, to illustrate the influence of the molecular brightness ϵ on the photon count distribution.

TABLE 1 PCH analysis of a fluorescein dilution experiment

c (nM)	c/[5.5 nM]	$\langle k \rangle$	$\langle k \rangle$/0.28	ϵ	$\bar{N}$	$\bar{N}$/0.347	Reduced χ^2
550	100	26.25	93.8	0.807	32.53	93.7	1.14
55	10	2.71	9.7	0.807	3.36	9.7	0.98
5.5	1	0.28	1.0	0.807	0.347	1.0	0.84

The photon counting histogram of fluorescein for three different concentrations was fitted globally to the theoretical PCH function $\Pi(k; \bar{N}, \epsilon)$. The molecular brightness ϵ was linked across the data sets, while the average number of molecules $\bar{N}$ was allowed to vary. The reduced χ^2 for each individual data set is shown in the table, with a global χ^2 of 1.01. The average number of photon counts per sampling period $\langle k \rangle$ was calculated directly from the experimental data. The ratios of the concentrations, the photon counts $\langle k \rangle$, and the number of molecules $\bar{N}$ were determined relative to the lowest concentration case.

Each fluorophore sample was made up to approximately the same concentration to facilitate the comparison of the different histograms. The count distributions were analyzed with the PCH algorithm and are shown together with the fits in Fig. 5. In addition, Poisson distributions with the same mean as the average photon counts are displayed as dashed lines for each histogram. The deviation between the tail of the PCH and the Poisson distribution increases with increasing ϵ, whereas for ϵ approaching zero the histogram converges to a Poisson distribution.

To demonstrate that the PCH of a mixture of two fluorescent species is given by the convolution of the individual histograms (Eq. 26), the following experiment was carried out. First the PCH distributions of fluorescein and cyanohydroxy-coumarin, each at a concentration of 1.2 nM, were obtained separately. In the next step, fluorescein and cyanohydroxy-coumarin were mixed together, such that each dye had a concentration of 1.2 nM. The PCH of the mixture was measured and is well represented by the convolution of the single species histograms, as shown in Fig. 6.

DISCUSSION

Fluctuations of a physical observable offer a convenient way to study microscopic processes and have proved useful in many fields (Weissman, 1981, 1988). FCS, for example, exploits the fluctuations of the fluorescence intensity in the time domain to recover details about the dynamics of molecules. Here we choose to study the same fluctuations in the amplitude domain instead of the time domain. The distribution of the amplitude fluctuations depends on the number of statistically independent contributions. In the one extreme, where many independent events contribute to the fluctuating signal, a Gaussian amplitude distribution is obtained regardless of the microscopic details. In this case the amplitude distribution describes ensemble properties, rather than the individual events. For FCS the other extreme applies, where only a few particles contribute to the fluorescence signal. The intensities are described by non-Gaussian statistics, which in principle allows us to extract information

TABLE 2 Comparison between PCH and autocorrelation analysis for a dilution series of rhodamine 110

C (nM)	$\langle k \rangle$	$\bar{N}_{g(\tau)}$	$\bar{N}_{PCH}$
10.8	4.76	10.70	12.82
5.4	2.28	6.03	6.15
2.7	1.11	3.13	2.99
1.35	0.57	1.59	1.55
0.68	0.29	0.81	0.78
0.34	0.16	0.48	0.44
0.17	0.085	0.29	0.23

For each dilution the photon count distribution and the autocorrelation were measured with a 40× Fluar objective (NA = 1.3) and a power at the sample of ~20 mW. The number of molecules in the excitation volume $\bar{N}_{PCH}$ was determined by a global fit of the histograms with the molecular brightness ϵ linked across the data sets. The average number of molecules $N_{g(\tau)}$ was determined by global analysis of the autocorrelation function $g(\tau)$ with the diffusion coefficient linked across the data sets. The average photon counts $\langle k \rangle$ were obtained directly from the experimental data.

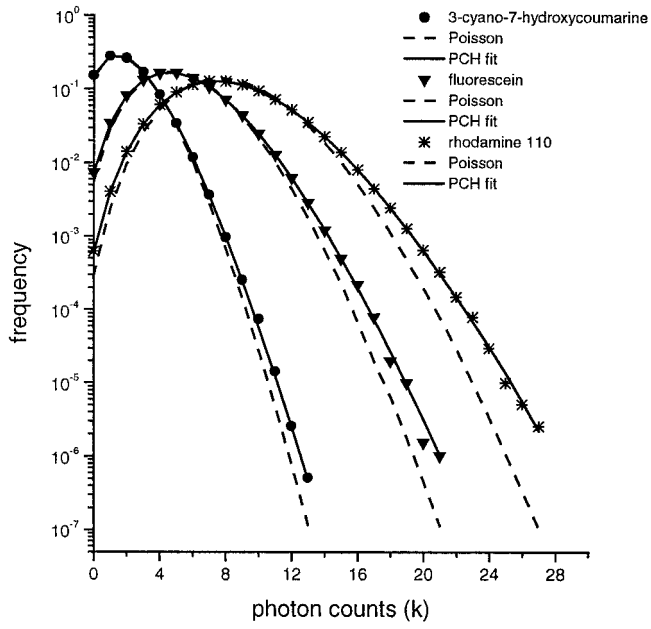

FIGURE 5 Photon counting histograms for three dyes, each with a different molecular brightness ϵ. The histograms of cyanohydroxycoumarin (●), fluorescein (▼), and rhodamine 110 (★), taken with the same number of data points, were fitted to the theoretical PCH function $\Pi(k; \bar{N}, \epsilon)$, shown as solid lines. The concentrations of the three samples were kept similar to each other to facilitate the comparison between the histograms. The fit recovered the average number of molecules $\bar{N}$ as 2.6, 3.3, and 3.0 for cyanohydroxycoumarin, fluorescein, and rhodamine 110, respectively. For the molecular brightness ϵ, values of 0.74 for cyanohydroxycoumarin, 1.60 for fluorescein, and 2.73 for rhodamine 110 were recovered. For each histogram a Poisson distribution with a mean equal to the average number of photon counts is plotted as a dashed line. The deviation between the Poisson distribution and the photon counting histogram increases markedly with increased molecular brightness ϵ.

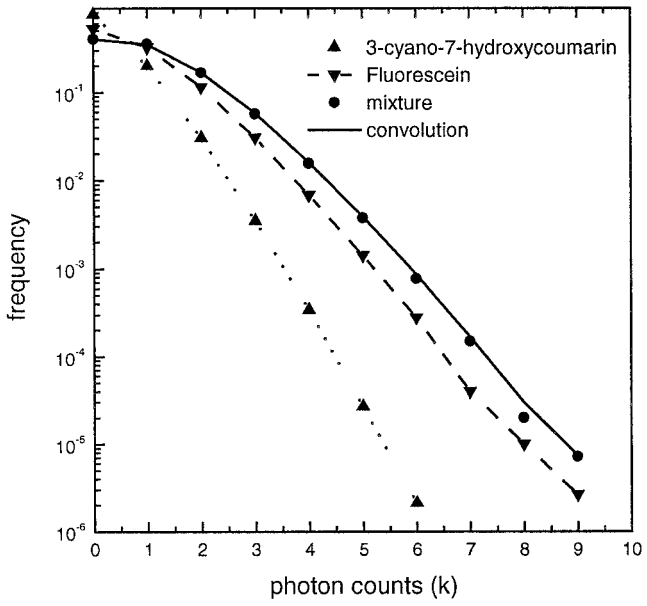

FIGURE 6 Photon counting histogram for fluorescein at 1.2 nM (▼), cyanohydroxycoumarin at 1.2 nM (▲), and a mixture of fluorescein and cyanohydroxycoumarin (●), each at a concentration of 1.2 nM. The solid line was determined by convoluting the experimental histograms of the individual dyes (*dashed lines* to guide the eye) and matches the photon counting histogram of the mixture.

about the individual fluorescent particles from the intensity distribution. The detection process needs additional consideration, because experimentally photon counts instead of intensities are measured. The photon count distribution still contains all of the information of the intensity distribution, but in a transformed manner. However, a well-developed theory relating the properties of the photon counts and intensities exists and had been applied in the past to study a variety of light sources (Bertolotti, 1973). Let us now consider the intensity fluctuations and their influence on the photon count distribution in more detail.

Three sources of fluctuations account for the shape of the photon counting histogram. The first one is a consequence of the quantum nature of the detection process. Because the absorption of a photon occurs almost instantaneously, no correlation between the atomic detector system and the electric field for adjacent photon counts exists. This noise generated by the detector is also known as shot noise and leads to a Poisson distribution of photon counts. The fluctuations of the fluorescent light intensity are caused by the diffusion of molecules in an inhomogeneous excitation profile and the particle number fluctuations within the observation volume, which represent the other two sources of noise. These intensity fluctuations introduce correlations between photon counts and are responsible for the super-Poissonian statistics of the photon count distribution as explained in the Theory section. FCS experiments always measure small, open volumes that freely exchange particles with the surrounding bath. The resulting number fluctuations of such a system alone are sufficient to cause non-Poissonian statistics. As an example, consider a homogeneous excitation profile, where the fluorescence intensity is not affected by the diffusion inside the observation volume. In this case the particle fluctuations lead to a compound Poisson distribution of photon counts:

$$\Pi(k; \bar{N}, \epsilon) = \sum_{N=0}^{\infty} p^{(N)}(k; V_{PSF}, \epsilon) p_{\#}(N) = \sum_{N=0}^{\infty} \mathrm{Poi}(k, \epsilon N)\mathrm{Poi}(N, \bar{N}). \tag{28}$$

The fact that the count distribution follows super-Poissonian instead of Poissonian statistics is crucial for extracting information from the histogram. Instead of one parameter, which is sufficient to characterize a Poisson distribution, two parameters, the average number of molecules in the excitation volume $\bar{N}$ and the brightness coefficient ϵ, are required to uniquely describe the single species histogram. The deviation of the PCH from a Poisson function is most pronounced in the tail of the distribution. Because the histogram values span several orders of magnitude, a logarithmic data representation as illustrated in Fig. 3 is necessary to make the super-Poissonian character of the PCH visible.

The photon counting histogram approaches a Poisson distribution with increasing fluorophore concentration, as shown in Fig. 3. This behavior can be readily understood by considering the influence of the molecule concentration on the intensity fluctuations. The relative strength of the number fluctuations is given by the ratio between the standard deviation σ and the mean μ of the molecule distribution:

$$\frac{\sigma}{\mu} = \frac{\sqrt{\langle \Delta N^2 \rangle}}{\bar{N}} = \frac{1}{\sqrt{\bar{N}}}. \tag{29}$$

The number of molecules inside a small, open volume is Poisson distributed, and the relative strength of the particle fluctuations decreases with the inverse square root of the average number of particles $\bar{N}$. Thus with increasing particle concentration the number distribution approaches a delta function $\delta(N - \bar{N})$. Consequently, the intensity fluctuations associated with the particle number die away. The second contribution to the intensity fluctuations, due to the diffusion in an inhomogeneous excitation profile, also vanishes at high particle concentrations; a vacancy created by a molecule leaving a position is almost always filled by another molecule moving to that position, so that no net change in the fluorescence intensity occurs. Thus the constant fluorescence intensity dictates a Poissonian photon count distribution.

To maximize the deviation between the photon count distribution and the corresponding Poisson function, one can either reduce the number of molecules within the excitation volume or increase the brightness parameter ϵ as demonstrated in Fig. 5. The relationship between the super-Poissonian character of the PCH and the molecular bright-

ness ϵ can be qualitatively understood. The average fluorescence intensity of a molecule in the excitation volume is characterized by the parameter ϵ. A particle with a larger value of ϵ causes stronger intensity fluctuations as it enters and diffuses through the beam. The increase in the fluorescence intensity fluctuations leads to a further broadening of the PCH. This behavior is a consequence of the averaging of Poisson distributions over a wider intensity range as expressed by Mandel's formula. To quantify this statement, we define the fractional deviation Q, a measure of the deviation between the PCH and the Poisson distribution (Mandel, 1979):

$$Q = \frac{\langle \Delta k^2 \rangle - \langle k \rangle}{\langle k \rangle} = \gamma \epsilon, \tag{30}$$

where $\langle \Delta k^2 \rangle$ and $\langle k \rangle$ are the variance and the expectation value of the photon counts, respectively. A Poissonian distribution is defined by $Q = 0$, whereas super-Poissonian distributions require $Q > 0$ and sub-Poissonian distributions mandate $Q < 0$. Q is directly proportional to the molecular brightness ϵ and the shape factor γ of the PSF, as shown in Appendix B. The γ factor is constant for a given PSF. Thus the super-Poissonian character of the PCH is largely determined by ϵ, which varies with the excitation power, the detection efficiency, and the molecular species.

Not all of the detected counts are due to the fluorophores of interest. Dark and background counts superimpose upon the photon counts from the actual sample. Background counts due to scattered light or sample contaminants can be largely suppressed by care in the sample preparation and the use of proper filters. Dark counts are inherent to all photon detectors; the details depend largely on the detector type, but cooling of the detector typically reduces the dark counts drastically. Under our experimental conditions, both the dark and background counts are on the order of 50 cps. The count rate of all measured samples exceeds 1000 cps; thus the influence of the dark and background counts on the PCH is negligible under these conditions. However, if necessary, it is straightforward to account for the dark and background signal. The dark and background events are statistically independent of the sample signal and act like an additional species. The PCH of this additional species can be determined separately and incorporated into the data fitting routine.

Far more serious than dark or background counts are intensity variations of the excitation source. Fluctuations of the excitation intensity induce fluctuations in the fluorescence intensity. The additional intensity fluctuations lead to a further broadening of the photon counting distribution. Hence, the fluorescence fluctuations are not independent of the excitation fluctuations, and there is no straightforward way to correct for this additional broadening. Care should be exercised to ensure a stable intensity output of the excitation source from the very beginning. We checked the excitation laser output (Fig. 1) to verify that the resulting PCH is described by a Poissonian distribution. The fact that the two-photon experiments require a pulsed excitation source with a repetition rate of $\sim$10 ns does not influence our experimental results, because we measure fluctuations in the microsecond to millisecond range. Intensity fluctuations of the excitation source, which occur on a time scale much faster than the sampling time T of the detector, are effectively averaged out and do not influence the counting statistics.

Generalization to more than one species has been described in the Theory section. In the case of two independent species, the corresponding PCH is obtained by convoluting the individual counting distributions of each species alone. If the two species interconvert chemically, they are no longer independent. Theoretically species interconversion would not affect the PCH, because all contributions from reactions vanish at $\tau = 0$ (Elson and Magde, 1974). In practice, however, we have to work with a short but finite sampling time T. In the limit that the integration time T is much smaller than the characteristic reaction time, the two species behave independently. In the other extreme, when the chemical interconversion time is much faster than the sampling time T, we will detect a single species with the time-averaged properties of the interconverting species. If the characteristic chemical reaction time is on the order of the sampling time T, then the additional fluorescence intensity fluctuations from the chemical reaction contribute to the counting statistics and consequently alter the counting histogram.

Both PCH and the autocorrelation function describe fluorescent fluctuations, but each focuses on a different property of the stochastic process. Whereas the autocorrelation function is a measure of the time-dependent decay of the fluctuations to their equilibrium value, the photon counting histogram captures the amplitude distribution of these fluctuations. Let us first consider a single fluorescent species as outlined in the Theory section. The autocorrelation function specifies the diffusion coefficient D. PCH, on the other hand, provides the average number of molecules $\bar{N}$ and the molecular brightness ϵ from the super-Poissonian character of the photon counts. The autocorrelation function $g(\tau)$ not only characterizes dynamic information, but also carries a static component, $g(0)$. The $g(0)$ value is inversely proportional to the average number of molecules $\bar{N}$, as shown by Eq. 32. The shot noise contribution to $g(0)$, however, makes it impossible to measure this value directly, and its value must be inferred by extrapolation of the fitted autocorrelation curve. From our experience both techniques, the autocorrelation and PCH, recover the average number of molecules $\bar{N}$ reliably. However, for dilutions the number of molecules $\bar{N}$ recovered by the PCH method scaled closest with the measured average photon counts $\langle k \rangle$ (see Table 2), suggesting a higher accuracy of the PCH method for our experimental conditions.

Resolving different species poses a practical and important problem. We will limit ourselves to the case of two species to facilitate the discussion. If the diffusion coefficient of two species differs substantially, then the two

species can be resolved by the autocorrelation approach. For small differences in the diffusion coefficient, resolving two species becomes exceedingly difficult and is often practically impossible. This is a serious limitation of the autocorrelation approach, because the diffusion coefficient is to a first approximation inversely proportional to the cube root of the molecular weight. Thus a wide class of biomolecules cannot be distinguished by diffusional analysis alone. One has to resort to more elaborate techniques like dual-color cross-correlation, which is able to separate based on the difference in the emission color of dyes (Schwille et al., 1997). Another approach to separating multiple species is higher order FCS, which has been described in detail in the literature (Palmer and Thompson, 1987, 1989b).

Here we want to discuss another approach based on PCH analysis. The PCH of a two-species sample is the convolution of the individual photon count distributions. Thus four parameters, the average number of molecules and the brightness of both species, are required to characterize the photon count distribution completely. The molecular brightness ϵ and the average number of molecules $\bar{N}$ shape the histogram distinctively, as discussed earlier. The convolution will change but still preserve the characteristics of each species. Thus as long as there is a brightness difference between the species, PCH will be able to resolve them, regardless of their diffusion coefficient. The demonstration and detailed analysis of this application will be the subject of a separate study.

CONCLUSION

In this paper we derived the theory of the photon counting histogram for fluorescence fluctuation experiments and constructed an algorithm to calculate the histogram numerically. The deviation of the probability function from Poissonian statistics is caused by the fluorescence intensity fluctuations due to the spatially inhomogeneous excitation profile of the laser beam and the fluorophore number fluctuations inside the excitation volume. Comparison between theory and experiment demonstrates that the data are in agreement with the theoretically predicted photon counting histograms. The PCH algorithm constitutes a novel analysis tool, as was demonstrated by extracting the average number of molecules within the excitation volume $\bar{N}$ and the molecular brightness ϵ from experimental data.

PCH is sensitive to the brightness of particles, thus offering a possibility to distinguish a mixture of species based on this feature alone. The autocorrelation function, on the other hand, is virtually insensitive to the brightness of molecules but sensitive to the time-dependent fluctuations in the fluorescence intensity. Thus PCH and FCS provide complementary information, which should prove useful for tackling biological problems with fluorescence fluctuation spectroscopy.

APPENDIX A

The probability $p^{(1)}(k; V_0, \epsilon)$ of detecting k photon counts for a single molecule diffusing within an enclosed volume V_0 depends on the size of the volume. If the reference volume is changed from V_0 to V_1, where $V_0 = fV_1$, the value of the probability of $p^{(1)}(k; V_0, \epsilon)$ must be transformed. We define the transformation of the probability $p^{(1)}(k; V, \epsilon)$ by changing the reference volume from V_0 to V_1 as

$$p^{(1)}(k; V_1, \epsilon) = fp^{(1)}(k; V_0, \epsilon) + (1 - f)\delta(k), \qquad (31)$$

with $\delta(k)$ as defined in Eq. 22.

If V_1 is larger than V_0, then $f = V_0/V_1$ represents the probability of finding the molecule inside the smaller volume V_0. The transformation of the probabilities by Eq. 31 represents the joint probability of finding the molecule inside the original volume V_0 with its probability distribution of photon counts $p^{(1)}(k; V_0, \epsilon)$ and the joint probability of finding the molecule outside the original volume $(1 - f)$ with its corresponding probability of photon counts. Because there is no excitation possible outside the volume V_0, the probability function for photon counts is given by $\delta(k)$.

In contrast to the probability of photon counts k for one molecule in a confined volume V_0, $p^{(1)}(k; V_0, \epsilon)$, the probability distribution $\hat{p}(k; V_0, \bar{N}, \epsilon)$ for the photon counts k of a freely diffusing chemical species with an average of $\bar{N}$ molecules in the volume V_0 is independent of the chosen reference volume. The independence of $\hat{p}(k; V_0, \bar{N}, \epsilon)$ from the arbitrary volume V_0 is intuitively expected, because $\hat{p}(k; V_0, \bar{N}, \epsilon)$ describes the probability of an open system. In this case, to describe the photon count probability for a different reference volume, one must consider that the average number of molecules scales with the size of the reference volume. For example, changing the volume from V_0 to V_1 changes the average number of molecules from $\bar{N}_0 \equiv \bar{N}$ to $\bar{N}_1 = \bar{N}_0/f$.

Now it is relatively straightforward to show that $\hat{p}(k; V_0, \bar{N}_0, \epsilon) = \hat{p}(k; V_1, \bar{N}_1, \epsilon)$, using Eqs. 20, 23, and 31. The choice of the auxiliary volume to calculate the probability of an open system is of no importance, as long as the average number of molecules $\bar{N}$ corresponds to the proper reference volume V. To reflect the independence from the reference volume, we define a new probability function for the open system $\Pi(k; \bar{N}_{PSF}, \epsilon)$, which by convention expresses the number of molecules $\bar{N}_{PSF}$ for the volume of the point spread function V_{PSF}.

In principle, any value for the auxiliary volume V_1 can be chosen to calculate the probability distribution $\Pi(k; \bar{N}_{PSF}, \epsilon)$, but practical considerations will limit the range of useful values. For very large volumes the average number of molecules $\bar{N}$ will also become very large, and the number of convolutions necessary to calculate the PCH becomes numerically cumbersome. By going to the other extreme and making the auxiliary volume V_1 very small, the function $p^{(1)}(k; V_1, \epsilon)$ loses its interpretation as a probability. The value of f in Eq. 31 would in this case be greater than 1, and the new value of $p^{(1)}(0; V_1, \epsilon)$ can be less than 0 and $p^{(1)}(1; V_1, \epsilon)$ greater than 1. But only the intermediate steps in the calculation lose their physical meaning. From a purely mathematical point of view, this is of no consequence for arriving at the final photon counting histogram $\Pi(k; \bar{N}_{PSF}, \epsilon)$, but should be avoided because of numerical problems. Values greater than 1 and less than 0 in $p^{(1)}(k; V_1, \epsilon)$ lead to increasing oscillations in the convolution (Eq. 20) to determine the function $\Pi(k; \bar{N}_{PSF}, \epsilon)$, which is numerically unstable. For practical purposes, using an auxiliary volume V_1 identical to the reference volume of the two-photon excitation V_{PSF} is typically a good compromise.

APPENDIX B

The fluorescence intensity autocorrelation function $g(\tau)$ at $\tau = 0$,

$$g(0) = \frac{\langle \Delta I^2 \rangle}{\langle I \rangle^2} = \frac{\langle \Delta k^2 \rangle - \langle k \rangle}{\langle k \rangle^2} = \frac{\gamma}{\bar{N}}, \qquad (32)$$

equates the ratio of the shape factor γ with the average number of molecules in the excitation volume $\bar{N}$ with the ratio of the variance $\langle \Delta I^2 \rangle$ to

the average $\langle I \rangle$ of the fluorescence intensity (Thompson, 1991). The shape factor γ,

$$\gamma = \frac{\int (\overline{\mathrm{PSF}}(\vec{r}))^2 \mathrm{d}\vec{r}}{\int \overline{\mathrm{PSF}}(\vec{r}) \mathrm{d}\vec{r}}, \tag{33}$$

depends on the functional form of the PSF. For the squared Gaussian-Lorentzian PSF, $\gamma = 3/(4\pi^2)$ (Berland et al., 1996). The moments of the fluorescence intensity and the moments of the photon counts are related to one another (Saleh, 1978). This relation is used to express $g(0)$ as a function of the variance $\langle \Delta k^2 \rangle$ and the average $\langle k \rangle$ of the photon counts. The subtraction of the average $\langle k \rangle$ from the variance $\langle \Delta k^2 \rangle$ eliminates the shot noise contribution to the photoelectron counts (Qian, 1990). The average photon counts $\langle k \rangle$ scale with the number of molecules present in the excitation volume $\bar{N}$ and the brightness per particle ϵ, so that $\langle k \rangle = \epsilon \bar{N}$, as derived in the Theory section. We can now express the fractional deviation Q by rewriting Eq. 32 as

$$Q = \frac{\langle \Delta k^2 \rangle - \langle k \rangle}{\langle k \rangle} = \gamma \epsilon. \tag{34}$$

We thank all members of the Laboratory for Fluorescence Dynamics for their help and encouragement.

This work was supported by the National Institutes of Health (RR03155) and the National Science Foundation (PHY95-13217).

REFERENCES

Aragon, S. R., and R. Pecora. 1975. Fluorescence correlation spectroscopy and Brownian rotational diffusion. *Biopolymers.* 14:119–137.

Bendat, J. S., and A. G. Piersol. 1971. Random Data: Analysis and Measurement Procedures. Wiley-Interscience, New York.

Berland, K. M., P. T. C. So, Y. Chen, W. W. Mantulin, and E. Gratton. 1996. Scanning two-photon fluctuation correlation spectroscopy: particle counting measurements for detection of molecular aggregation. *Biophys. J.* 71:410–420.

Berland, K. M., P. T. C. So, and E. Gratton. 1995. Two-photon fluorescence correlation spectroscopy: method and application to the intracellular environment. *Biophys. J.* 68:694–701.

Bertolotti, M. 1973. Photon statistics. *In* Photon Correlation and Light Beating Spectroscopy. H. Z. Cummins and E. R. Pike, editors. Plenum Press, New York. 41–74.

Borejdo, J. 1979. Motion of myosin fragments during actin-activated ATPase: fluorescence correlation spectroscopy study. *Biopolymers.* 18: 2807–2820.

Braun, H. A., H. Wissing, K. Schafer, and M. C. Hirsch. 1994. Oscillation and noise determine signal transduction in shark multimodal sensory cells. *Nature.* 367:270–273.

Chandrasekhar, S. 1943. Stochastic problems in physics and astronomy. *Rev. Mod. Phys.* 15:1–89.

Ehrenberg, M., and R. Rigler. 1974. Rotational Brownian motion and fluorescence intensity fluctuations. *Chem. Phys.* 4:390–401.

Eigen, M., and R. Rigler. 1994. Sorting single molecules: application to diagnostics and evolutionary biotechnology. *Proc. Natl. Acad. Sci. USA.* 91:5740–5747.

Elson, E. L., and D. Magde. 1974. Fluorescence correlation spectroscopy. I. Conceptual basis and theory. *Biopolymers.* 13:1–27.

Feller, W. 1957. An Introduction to Probability Theory and Its Applications. John Wiley and Sons, New York.

Glauber, R. J. 1966. *In* Physics of Quantum Electronics. P. L. Kelley, B. Lax, and P. E. Tannenwald, editors. McGraw-Hill, New York. 788.

Kask, P., P. Piksarv, M. Pooga, and Ü. Mets. 1989. Separation of the rotational contribution in fluorescence correlation experiments. *Biophys. J.* 55:213–220.

Kimble, H. J., M. Dagenais, and L. Mandel. 1977. Photon antibunching in resonance fluorescence. *Phys. Rev. Lett.* 39:691–695.

Kinjo, M., and R. Rigler. 1995. Ultrasensitive hybridization analysis using fluorescence correlation spectroscopy. *Nucleic Acids Res.* 23: 1795–1799.

Koppel, D. E. 1974. Statistical accuracy in fluorescence correlation spectroscopy. *Phys. Rev. A.* 10:1938–1945.

Koppel, D. E., D. Axelrod, J. Schlessinger, E. L. Elson, and W. W. Webb. 1976. Dynamics of fluorescence marker concentration as a probe of mobility. *Biophys. J.* 16:1315–1329.

Koppel, D. E., F. Morgan, A. E. Cowan, and J. H. Carson. 1994. Scanning concentration correlation spectroscopy using the confocal laser microscope. *Biophys. J.* 66:502–507.

Magde, D., E. Elson, and W. W. Webb. 1972. Thermodynamic fluctuations in a reacting system: measurement by fluorescence correlation spectroscopy. *Phys. Rev. Lett.* 29:705–708.

Magde, D., E. L. Elson, and W. W. Webb. 1974. Fluorescence correlation spectroscopy. II. An experimental realization. *Biopolymers.* 13:29–61.

Magde, D., W. W. Webb, and E. L. Elson. 1978. Fluorescence correlation spectroscopy. III. Uniform translation and laminar flow. *Biopolymers.* 17:361–376.

Mandel, L. 1958. Fluctuations of photon beams and their correlations. *Proc. Phys. Soc.* 72:1037–1048.

Mandel, L. 1979. Sub-Poissonian photon statistics in resonance fluorescence. *Optics Lett.* 4:205–207.

Mandel, L., and E. Wolf. 1995. Optical Coherence and Quantum Optics. Cambridge University Press, Cambridge.

Palmer, A. G., III, and N. L. Thompson. 1987. Molecular aggregation characterized by high order autocorrelation in fluorescence correlation spectroscopy. *Biophys. J.* 52:257–270.

Palmer, A. G., and N. L. Thompson. 1989a. Fluorescence correlation spectroscopy for detecting submicroscopic clusters of fluorescent molecules in membranes. *Chem. Phys. Lipids.* 50:253–270.

Palmer, A. G. D., and N. L. Thompson. 1989b. High-order fluorescence fluctuation analysis of model protein clusters. *Proc. Natl. Acad. Sci. USA.* 86:6148–6152.

Qian, H. 1990. Inverse poisson transformation and shot noise filtering. *Rev. Sci. Instrum.* 61:2088–2091.

Qian, H., and E. L. Elson. 1989. Characterization of the equilibrium distribution of polymer molecular weights by fluorescence distribution spectroscopy (theoretical results). *In* Applied Polymer Symposia. John Wiley and Sons, New York. 305–314.

Qian, H., and E. L. Elson. 1990. Distribution of molecular aggregation by analysis of fluctuation moments. *Proc. Natl. Acad. Sci. USA.* 87: 5479–5483.

Qian, H., and E. L. Elson. 1991. Analysis of confocal laser-microscope optics for 3-D fluorescence correlation spectroscopy. *Appl. Opt.* 30: 1185–1195.

Rabin, M. W., R. D. Merithew, M. B. Weissman, M. J. Higgins, and S. Bhattacharya. 1998. Noise probes of underlying static correlation lengths in the superconducting peak effect. *Phys. Rev. B.* 57:720–723.

Rauer, B., E. Neumann, J. Widengren, and R. Rigler. 1996. Fluorescence correlation spectrometry of the interaction kinetics of tetramethylrhodamin alpha-bungarotoxin with *Torpedo californica* acetylcholine receptor. *Biophys. Chem.* 58:3–12.

Rigler, R., Ü. Mets, J. Widengren, and P. Kask. 1993a. Fluorescence correlation spectroscopy with high count rate and low background: analysis of translational diffusion. *Eur. Biophys. J.* 22:169–175.

Rigler, R., J. Widengren, and Ü. Mets. 1993b. Interactions and kinetics of single molecules as observed by fluorescence correlation spectroscopy. *In* Fluorescence Spectroscopy: New Methods and Applications. O. S. Wolfbeis, editor. Springer-Verlag, Berlin. 13–24.

Saleh, B. 1978. Photoelectron Statistics, with Applications to Spectroscopy and Optical Communications. Springer-Verlag, Berlin.

Schwille, P., F. J. Meyer-Almes, and R. Rigler. 1997. Dual-color fluorescence cross-correlation spectroscopy for multicomponent diffusional analysis in solution. *Biophys. J.* 72:1878–1886.

Schwille, P., F. Oehlenschlager, and N. G. Walter. 1996. Quantitative hybridization kinetics of DNA probes to RNA in solution followed by

diffusional fluorescence correlation analysis. *Biochemistry.* 35: 10182–10193.

Short, R., and L. Mandel. 1983. Observation of sub-Poissonian photon statistics. *Phys. Rev. Lett.* 51:384–387.

Siedentopf, H., and R. Zsigmondy. 1903. Über die Sichtbarmachung und Grössenbestimmung ultramikroskopischer Teilchen, mit besonderer Anwendung auf Goldrubingläser. *Ann. Phys. [4].* 10:1–39.

Snyder, D. L. 1975. Random Point Processes. Wiley-Interscience, New York.

Teich, M. C., and B. E. A. Saleh. 1988. Photon bunching and antibunching. *In* Progress in Optics. E. Wolf, editor. North-Holland Publishing Company, Amsterdam. 1–104.

Thompson, N. L. 1991. Fluorescence correlation spectroscopy. *In* Topics in Fluorescence Spectroscopy. J. R. Lakowicz, editor. Plenum, New York. 337–378.

Thompson, N. L., and D. Axelrod. 1983. Immunoglobulin surface-binding kinetics studied by total internal reflection with fluorescence correlation spectroscopy. *Biophys. J.* 43:103–114.

van Kampen, N. G. 1981. Stochastic Processes in Physics and Chemistry. Elsevier North-Holland, New York.

Walls, D. F. 1983. Squeezed states of light. *Nature.* 306:141–146.

Weissman, M. B. 1981. Fluctuation spectroscopy. *Annu. Rev. Phys. Chem.* 32:205–232.

Weissman, M. B. 1988. 1/*f* noise and other slow, nonexponential kinetics in condensed matter. *Rev. Mod. Phys.* 60:537–571.

Weissman, M. B. 1993. What is a spin glass? A glimpse via mesoscopic noise. *Rev. Mod. Phys.* 65:829–839.

Widengren, J., Ü. Mets, and R. Rigler. 1995. Fluorescence correlation spectroscopy of triplet states in solution—a theoretical and experimental study. *J. Phys. Chem.* 99:13368–13379.